

Normalized Landslide Index Method for susceptibility map development in El Salvador

Ari J. Posner¹ · Konstantine P. Georgakakos^{1,2}

Received: 18 June 2014 / Accepted: 7 August 2015 / Published online: 22 August 2015
© Springer Science+Business Media Dordrecht 2015

Abstract El Salvador and Central America in general are highly prone to landsliding. In November 1998, Hurricane Mitch killed 240 people, displaced about 85,000 people, caused more than \$600 million in economic losses, and damaged about 60 % of the nation's roads (Rose et al. in *Natural hazards in El Salvador*. Geologic Society of America of special paper 375, Boulder, 2004). An understanding of susceptibility of locations to landsliding is critical for development and mitigation planning. This work presents the development of the Normalized Landslide Index Method which is a derivative of the bivariate statistical methods commonly used in landslide susceptibility assessment. The resultant map was amended through a tangential analysis, also commonly used in landslide susceptibility mapping, the Analytical Hierarchy Process (AHP), which reduces multi-criteria analysis to pair-wise comparisons. The assimilation of results from the AHP analysis into the statistically derived susceptibility map skewed the original results by emphasizing the extremes already found. It was determined that addition of AHP results did not increase the value of the derived susceptibility map. Finally, a physically based a priori approach to landslide susceptibility mapping, developed by El Salvador National Service of Territorial Studies, was compared to the statistically derived map developed herein. It was found that the a priori approach was not sufficiently discriminant to be useful for planners and regulators, as very large areas were designated high susceptibility that included areas with low slope angles. The development of the normalized landslide index is a significant improvement to the class of bivariate statistical strategies to assess regional landslide susceptibility.

Keywords Landslide susceptibility · Analytical Hierarchy Process · Landslide index method · Bivariate statistics · El Salvador

✉ Ari J. Posner
aposner@hrcwater.org

¹ Hydrologic Research Center, 12555 High Bluff Drive, Suite 255, San Diego, CA 92130, USA

² Scripps Institution of Oceanography, University of California at San Diego, La Jolla, CA 92093, USA

1 Introduction

Shallow landslides are triggered by rainfall events of high intensity and short duration. Although landslides may occur in small portions of a hilly or mountainous landscape, their impact to the safety and well-being of inhabitants and the local economy is disproportionately felt (Meisina et al. 2013). The necessity to identify landslide-prone areas at the regional scale is critical to plan mitigation measures and to alert populations during extreme rainfall events.

Landslide susceptibility and/or hazard mapping has evolved dramatically with the widespread availability of geographic information system technology and the availability of spatial datasets including land classification and other information from remote sensing. Methodologies for the development of landslide susceptibility maps can be divided into *statistical methods* that use the locations of existing landslides along with land classification databases for statistical analysis and *physically based methods* that predict landslide susceptibility independent of the locations of previous landslide events and rely solely on land, climate, and in some cases seismic activity geo-spatial classifications (Van Den Eeckhaut et al. 2006). There are advantages and disadvantages to each strategy. Statistical models are primarily limited due to the fact that the conceptual model on which they are founded is that “the past (and present) landslide locations are the key to the future” (Carrara et al. 1995; Zêzere 2002). The accuracy and precision of physically based methods are highly dependent upon the detail of available climatologic, hydrologic, and geomorphologic temporally and spatially distributed datasets.

Approaches to landslide hazard/susceptibility mapping have evolved and now include bivariate, multivariate logistic regression, fuzzy logic, and artificial neural network analysis (van Westen 1997; Dai et al. 2001; Lee and Min 2001; Ercanoglu and Gokceoglu 2004; Lee et al. 2004a, b; Komac 2006). A promising strategy comes from the Wharton School of Business in the form of a decision-making tool known as the Analytical Hierarchy Process (Saaty 1980). Yalcin (2008) compared the use of Analytical Hierarchy Process (AHP) with two other commonly used methods for landslide susceptibility mapping: the statistical index and waiting factor methods, and found that the Analytical Hierarchy Process did significantly better than the statistical methods employed at predicting the locations of known landslides based on topographic and geomorphologic features.

This paper describes the development of a statistical-based landslide susceptibility map, which is subsequently refined using subjective criteria developed through use of the AHP. The susceptibility map weights are compared both before and after implementation of AHP, in order to assess the impact of its assimilation. Then, the statistically based developed susceptibility map is compared to a physically based susceptibility map that was developed by the El Salvador National Service of Territorial Studies (SNET).

2 Study area

The region of Central America is very prone to natural hazards (Rose et al. 2004). El Salvador is located on the western side of Central America, and it is bounded by the Pacific Ocean to the west, the Río Sumpul to the east on its border with Honduras, the Río Paz on the northern border with Guatemala, and the Río Goascorán on the southern border with Nicaragua. Despite being Central America’s smallest country in area (21,040 km²), El Salvador has the highest population density (~290 persons/km²).

As a consequence of lying above the subduction zone between the Cocos and Caribbean tectonic plates, El Salvador is bisected by a linear belt of active volcanoes and associated seismic zones, a coastal plain lying to the south and rolling mountains to the north (Rose et al. 2004). The bedrock geology of much of El Salvador is unknown due to extensive volcanic activity and the associated pyroclastic flows that cover much of the country with ignimbrites up to 650 m thick (Baxter 1984). Geological surveying shows that the country is composed of volcanic rocks, with a few exceptions (Fig. 1). With respect to landslide susceptibility, these minerals are easily weathered to illite and smectite clays, which create slip surfaces for overlying deposits.

The territory of El Salvador has pronounced relief, with four mountain chains of broken and rugged terrain. Mountain chains include the coastal chain that parallels the coast separated by alluvial plains comprising three separate masses that represent about 13 % of the country's total land mass. At approximately 12 % of the total area, the young volcanos of Apaneca-Lamatpepc, San Salvador, San Vicente, Tecapa-San Miguel, and Conchagua include calderas, high plains, and deeply eroded slopes. The country is also bisected by a graben extending from east to west, characterized by steep slopes from 30 to 50 %. Finally, in the northern part of the country, three large groups of mountains define the border with Honduras and Guatemala, with the country's tallest mountain at 2730 m.

At approximately 13° north latitude, El Salvador lies just north of the northernmost migration site of Intertropical Convergence Zone (ITCZ) in Central America. Here, a well-defined annual cycle of precipitation is characterized by a rainy season from May to October, with the remainder of the year being dry (Aguilar et al. 2009). The passage of transient weather disturbances across the region is the result of meridional displacements of the ITCZ, and the passage of hurricanes, tropical storms and depressions, and easterly waves. Caribbean easterly waves are the most common disturbance, with approximately 60 tropical waves per year reaching the eastern part of Central America (Pasch et al. 1998). Hurricanes and tropical depressions, when combined with the steep mountainous terrain, primarily volcanic soils, and high population densities, have resulted in major loss of life, the most recent example being the landfall of Hurricane Mitch during 1998 (Hellin et al. 1999; Bell et al. 1999).

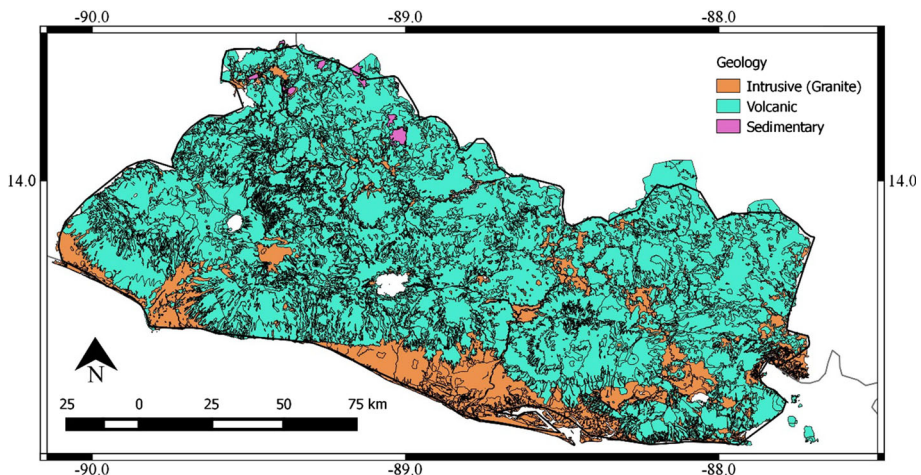


Fig. 1 Broad geologic categories across El Salvador

In the aftermath of Hurricane Mitch, the government of El Salvador created the Servicio Nacional de Estudios Territoriales (SNET) to monitor seismic activity and investigate landslides and landslide susceptibility. The SNET database includes a geo-referenced database of 260 landslide occurrences dating from 1762 to August 2012. Of the 260 landslides, according to the database, 113 were rain-induced (Fig. 2).

In order to verify the locations of each landslide, point locations were entered into Google Earth, where aerial imagery could be used to identify actual landslide locations. In addition, field notes for each landslide location were reviewed along with historical aerial imagery also available in Google Earth. Through this process, many of the point locations were removed due to the fact that they were located within a municipality. This process also permitted the delineation of polygons associated with the head escarpments of landslide locations. This delineation process resulted in the identification of 545 distinct polygons (Fig. 2).

Data used in the development of susceptibility maps for El Salvador were limited by the spatial resolution of the digital elevation model which is used to generate several geometric characteristics of interest such as slope, aspect, tangential and profile curvatures. The resolution of the available DEM is $30\text{ m} \times 30\text{ m}$; therefore, all other variables were transformed to this resolution. Delineated landslide polygons were converted to this gridded representation resulting in 1231 grid cells (approximately 1 sq km total) where landslides had occurred.

3 Landslide susceptibility mapping

3.1 Normalized Landslide Index Method

In order to identify what areas are most susceptible, or have the highest risk, of future landsliding, the historic landslide database provided by SNET was used. In addition to

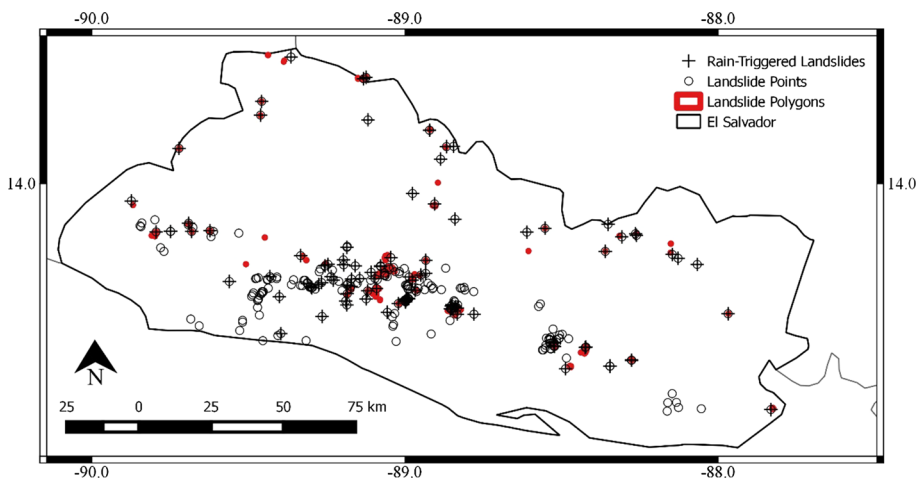


Fig. 2 All documented landslides by SNET with those rain-induced landslides identified. Landslide head scarp polygons verified through aerial images and field visit report review, polygon sizes exaggerated so as to be visible

landslide point locations, additional attributes were provided such as the timing of the landslide and the triggering mechanism (seismic or rain-induced), and in some cases a field visit report were also available for review.

In selecting the causal factors for any geo-spatial investigation, Yalcin (2008) identified five criteria researchers should ensure: (1) operational (has a certain degree of affinity with the dependent variable, in this case landslide location), (2) complete (is represented across the entire domain), (3) non-uniform (varies spatially), (4) measurable (can be expressed by nominal, ordinal, interval, or ratio scales), and (5) and non-redundant (its effect should not account for double consequences in the final result). Geo-spatial variables such as lithology-weathering, distance to streams and roads, and land cover classes, along with DEM-derived variables such as slope, aspect, plan, and profile curvatures, are commonly used to derive landslide susceptibility researchers (Dai et al. 2001, 2002; Lee and Min 2001; Parise 2001; Cevik and Topal 2003; Lee et al. 2004a, b; Lan et al. 2004; Perotto-Baldiviezo et al. 2004; Ayalew et al. 2005; Ayalew and Yamagishi 2005; Komac 2006). Continuous variables such as topographic slope must be classified into discrete classes for further analysis (see Table 2). The aspect variable was broken into six classes based on their orientation, with 0° representing directly east and moving around clockwise at 60° intervals. The remaining continuous variables, slope, and tangential and profile curvatures were classified by dividing all of the values into five equal size bins.

The core of the bivariate statistical analysis undertaken is an overlay of parameter maps and calculations of landslide densities in order to assess the importance of each parameter. By normalizing values, using the landslide density per parameter class in relation the landslide density over the entire area, a total hazard map is created by the addition of weights for individual parameters. The bivariate statistical analysis performed is often referred to as the statistical or landslide index method (subsequently referred to as the index method). In the index method, a weight value for a parameter class is defined as the natural logarithm of the landslide density class, divided by the landslide density over the entire map (van Westen 1997; Yalcin 2008; Rautela and Lakhera 2000; Quinn et al. 2010). This is done using Eq. (1),

$$W_i = \ln\left(\frac{\text{Landslide Class Density}}{\text{Landslide Map Density}}\right) = \ln\left(\frac{\frac{N_{\text{pix}}(S_i)}{N_{\text{pix}}(N_i)}}{\sum \frac{N_{\text{pix}}(S_i)}{N_{\text{pix}}(N_i)}}\right) \tag{1}$$

where W_i , the weight given to a certain parameter class (i) (e.g., lithology, slope, etc.); $N_{\text{pix}}(S_i)$, number of pixels, which contain landslides, in a certain parameter class; and $N_{\text{pix}}(N_i)$, total number of pixels in a certain parameter class.

Taking the natural logarithm of this relative density results in positive values where landslides are highly represented in any given parameter class and negative values where landslides are poorly represented. The index method is based on statistical correlation (map crossing) of different parameter maps and the landslide inventory map with parameter class attributes. Preprocessing of spatially distributed variables included the processing of a digital elevation model to derive slope, aspect, profile, and tangential curvature categories. These continuous variables were then divided into discrete classes (see Tables 1, 2, 3, 4, 5, 6, 7). Polygon vector geo-spatial representations of land use and geology were first lumped into fewer classes by combining distinct classes, as there were 61 and 25 classes in the original data provided by SNET, respectively (Tables 5, 6). After lumping classes based on general characteristics, vectors were converted to raster-based representations to achieve spatial continuity between all parameters. Each weight class was then normalized to the

normal of classes in the parameter, as parameters such as land use, that have twice the number of classes as slope; for example, weights were misrepresented in the final susceptibility map due to the dilution of weight value from not having the same number of classes in each parameter.

In the present study, each parameter map was crossed with the landslide inventory map, and the density of the landslides in each class was calculated. Correlation results were stored in resultant rasters, and the density of the landslide per parameter class was calculated. Then, the parameter weight ($\ln W_i$) value of each attribute was calculated (Tables 1, 2, 3, 4, 5, 6, 7; Fig. 3). Finally, all layers were overlaid and a resultant susceptibility map was obtained by summing the weights for each parameter (Fig. 3). The final susceptibility map was divided into equal classes according to the total number of elements. The classes are: low, medium, high, and very high susceptibility (Fig. 3).

Geo-spatial and statistical analysis were implemented through a combination of the Quantum GIS (QGIS Development Team 2014), GRASS GIS (GRASS Development Team 2012); MATLAB (2012); Microsoft Excel (2010).

3.2 Results

3.2.1 Slope factor

The slope factor was divided into five classes, with an equal number of pixels in each. Results from the analysis indicate that representation of landslides in any given class is significantly greater as slopes increase. Landslides are 3.7 times more likely to be represented in the steepest slope class than the lowest slopes according to this analysis.

3.2.2 Aspect factor

The aspect factor was divided into six equal classes. Aspect class ranges represent degrees in a counterclockwise direction with 0° representing due east. Class discrimination was decided based on the orientation of primary mountain chains in the region that extend in a northwest to southeasterly direction. Weights for any particular aspect class are small with no particularly strong signal coming from any direction. The aspects where landslides are positively represented are those facing north and northeast.

Table 1 Variable class values from spatial domain of interest and weight calculations for slope

Slope	n (pix)	LS $_n$ (pix)	Weight	LN (weight)	Normalized LN (weight)	AHP factor (wt)	Actual (wt)
0–3.332	4,534,045	11	0.045	–3.108	–0.62165	0.52200	–0.32450
3.332–6.4813	4,534,050	55	0.223	–1.499	–0.29976	0.52200	–0.15648
6.4813–11.0874	4,534,062	125	0.508	–0.678	–0.13557	0.52200	–0.07077
11.0874–18.0498	4,534,054	197	0.800	–0.223	–0.04459	0.52200	–0.02328
>18.0498	4,534,054	843	3.424	1.231	0.24616	0.52200	0.12850
Sum	22,670,265	1231					

Table 2 Variable class values from spatial domain of interest and weight calculations for aspect

Aspect	<i>n</i> (pix)	LS_ <i>n</i> (pix)	Weight	LN (weight)	Normalized LN (weight)	AHP factor (wt)	Actual (wt)
0–59	3,930,630	215	1.002	0.002	0.00032	0.02929	0.00001
60–119	3,307,953	162	0.897	–0.109	–0.01811	0.02929	–0.00053
120–179	3,477,120	122	0.643	–0.442	–0.07368	0.02929	–0.00216
180–239	4,004,849	208	0.951	–0.050	–0.00831	0.02929	–0.00024
240–299	3,930,674	248	1.156	0.145	0.02412	0.02929	0.00071
300–359	3,842,172	273	1.301	0.264	0.04392	0.02929	0.00129
Sum	22,493,398	1228					

Table 3 Variable class values from spatial domain of interest and weight calculations for profile curvature

Profile curvature	<i>n</i> (pix)	LS <i>n</i> (pix)	Weight	LN (weight)	Normalized LN (weight)	AHP factor (wt)	Actual (wt)
<–0.0028	4,534,053	257	1.044	0.043	0.00859	0.04480	0.00038
–0.0028 to –0.00085	4,534,053	179	0.727	–0.319	–0.06375	0.04480	–0.00286
–0.00085 to 0.0006	4,534,053	155	0.630	–0.463	–0.09254	0.04480	–0.00415
0.0006–0.0026	4,534,053	221	0.898	–0.108	–0.02160	0.04480	–0.00097
>0.0026	4,534,053	419	1.702	0.532	0.10635	0.04480	0.00476
Sum	22,670,265	1231	1				

Table 4 Variable class values from spatial domain of interest and weight calculations for tangential curvature

Tangential curvature	<i>n</i> (pix)	LS <i>n</i> (pix)	Weight	LN (weight)	Normalized LN (weight)	AHP factor (wt)	Actual (wt)
<–0.0026	4,534,053	418	1.698	0.529	0.10587	0.08337	0.00883
–0.0026 to –0.0006	4,534,053	158	0.642	–0.444	–0.08871	0.08337	–0.00740
–0.0006 to 0.00079	4,534,053	138	0.561	–0.579	–0.11578	0.08337	–0.00965
0.00079–0.0028	4,534,053	179	0.727	–0.319	–0.06375	0.08337	–0.00531
>0.0028	4,534,053	338	1.373	0.317	0.06338	0.08337	0.00528
Sum	22,670,265	1231					

3.2.3 Profile curvature factor

Profile curvature represents the concavity or convexity of a slope in the down slope direction (Fig. 4). Classes in the profile curvature parameter were divided into five discrete classes representing planar, moderate, and high positive or negative profile curvature. Classes were determined based on an equal number of pixels in each class bin. Results indicate that landslides are slightly better represented in locations with high profile

Table 5 Variable class values from spatial domain of interest and weight calculations for lithology

Lithology	<i>N</i> (pix)	LS <i>N</i> (pix)	Weight	LN (weight)	Normalized LN (weight)	AHP factor (wt)	Actual (wt)
Limestones and marly limestones	15,823	20	23.298	3.148	0.12593	0.1998	0.02516
Cones of accumulation (slag, lapilli tuffs, cinder)	79,957	116	26.741	3.286	0.13145	0.1998	0.02627
Effusive basic-intermediate	3,433,106	1	0.005	-5.227	-0.20909	0.1998	-0.04178
Basic-intermediate effusive, subordinate pyroclastic	3,550,245	36	0.187	-1.677	-0.06709	0.1998	-0.01341
Effusive basic-intermediate, pyroclastic, volcanic epiclasts	859,690	335	7.183	1.972	0.07887	0.1998	0.01576
Intermediate to acidic effusive pyroclastic intermediate	728,350	16	0.405	-0.904	-0.03616	0.1998	-0.00723
Volcanic and pyroclastic; -basic-intermediate effusive	2,247,609	90	0.738	-0.304	-0.01215	0.1998	-0.00243
Acidic to intermediate pyroclastic	2,778,823	12	0.080	-2.531	-0.10123	0.1998	-0.02023
Pyroclastic acidic, volcanic epiclasts	2,585,239	51	0.364	-1.012	-0.04047	0.1998	-0.00809
Pyroclastic acidic, epiclasts volcanic (tuffs brown color)	1,992,580	4	0.037	-3.297	-0.13187	0.1998	-0.02635
Pyroclastic acidic, ignimbrites, volcanic epiclasts	1,399,731	82	1.080	0.077	0.00307	0.1998	0.00061
Acidic to intermediate intrusive rocks	85,263	15	3.243	1.176	0.04706	0.1998	0.00940
White Earth acidic volcanic and subordinate pyroclastic	599,576	452	13.895	2.632	0.10526	0.1998	0.02103
SUM	22,689,883	1231					

curvatures, whether positive or negative, but almost an order of magnitude better represented in positively curved slopes.

3.2.4 Tangential curvature factor

Tangential curvature refers to the degree to which any given pixel is surrounded by pixels that either feed into, or out of that pixel, hydrologically. Classes in the tangential curvature parameter were also divided into five discrete classes representing planar, moderate, and high positive or negative tangential curvature. Similar to the profile curvature, there is a

Table 6 Variable class values from spatial domain of interest and weight calculations for land use

Land use	<i>N</i> (pix)	LS <i>N</i> (pix)	Weight	LN (weight)	Normalized LN (weight)	AHP factor (wt)	Actual (wt)
Evergreen forests	288,707	31	1.9116	0.6479	0.0127	0.12072	0.0015
Coniferous forests	565,469	4	0.1259	−2.0720	−0.0406	0.12072	−0.0049
Mixed forests	153,626	73	8.4595	2.1353	0.0419	0.12072	0.0051
Coffee plantations	2,433,579	370	2.7067	0.9957	0.0195	0.12072	0.0024
Annual crops	797,478	9	0.2009	−1.6049	−0.0315	0.12072	−0.0038
Basic grains	3,451,866	361	1.8618	0.6216	0.0122	0.12072	0.0015
Mosaic of pasture and farms	1,589,433	18	0.2016	−1.6014	−0.0314	0.12072	−0.0038
Natural pasture	1,781,610	2	0.0200	−3.9128	−0.0767	0.12072	−0.0093
Lava, rock	51,517	73	25.2266	3.2279	0.0621	0.12072	0.0075
Continuous urban fabric	269,109	57	3.7708	1.3273	0.0255	0.12072	0.0031
Discontinuous urban fabric	134,408	8	1.0596	0.0579	0.0011	0.12072	0.0001
Principally agricultural lands	2,599,934	18	0.1233	−2.0935	−0.0403	0.12072	−0.0049
Low shrubs	822,877	5	0.1082	−2.2240	−0.0428	0.12072	−0.0052
Herbaceous natural vegetation	291,062	77	4.7097	1.5496	0.0298	0.12072	0.0036
SUM	19,707,584	1107					

Table 7 Satty’s Scale for Comparison

Scales	Degree of preference	Explanation
1	Equally	Two activities contribute equally
3	Moderately	Experience and judgment slightly to moderately favor one activity to another
5	Strongly	Experience and judgment strongly or essentially favor one activity over another
7	Very strongly	One activity is strongly favored over another, and its dominance is showed in practice
9	Extremely	The evidence of favoring one activity over another is of the highest degree possible of an affirmation
2, 4, 6, 8	Intermediate values	Used to represent compromises between the preferences in weights 1, 3, 5, 7, and 9
Reciprocals	Opposites	Used for inverse comparisons

slight positive correlation to the high tangential curvatures in both the positive and negative directions, with landslides being much better represented in negatively curved tangential slopes Fig. 5.

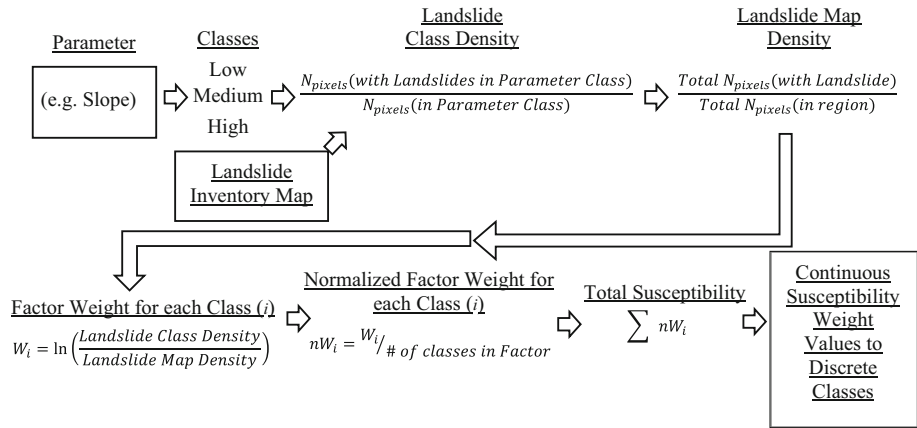


Fig. 3 Flow chart of development of normalized landslide index landslide susceptibility map

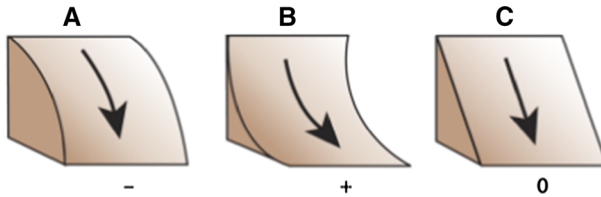


Fig. 4 Profile curvature diagram to illustrate positive and negative values

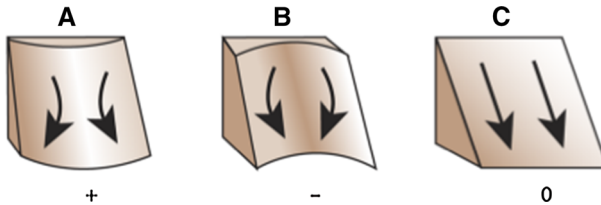


Fig. 5 Tangential curvature diagram to illustrate positive and negative values

3.2.5 *Lithology factor*

The lithology factor classes were not altered from the data provided by SNET. In general, all of the area can be described as volcanic. However, this analysis shows that landslide locations are significantly more likely to occur in volcanic cones and White Earth volcanic epiclasts than any other lithology class type. In addition, there are two lithology classes that are equally significant in their underrepresentation with landslides, basic-intermediate epiclasts and brown color tuffs.

3.2.6 *Land use factor*

Of the 60 land use classes used to classify El Salvador by SNET, 14 of them contained landslides. Of these 14 classes that contained landslides, eight classes are well represented,

with positive weight values, and six poorly represented with negative normalized weight values. Normalization of LN weights based on the number of variable classes has a dramatic impact on land use weights by reducing them significantly, making positive values less positive and negative values less negative.

3.2.7 Normalized Landslide Index Method landslide susceptibility map

Each pixel in the spatial domain was given a total landslide hazard susceptibility weight calculated by the sum of each variable class weight in each cell from Eq. (1) (Tables 1, 2, 3, 4, 5, 6; Column “Normalized LN Weight”). Figure 6 shows the cumulative probability of LN (Weights) and normalized weights across the entire domain, along with the values at landslide locations. Figure 6 illustrates that normalization of variable class weights results in a more even distribution of weights across the range of values, with shorter tails on each end of the cumulative probability plot.

In order to assess the relative importance of any given parameter and the particular class within that parameter, Fig. 7 is a plot of the results of the normalized and standard landslide index method analyses Figure 7 illustrates that slope and lithology are the strongest predictors of landslide location, with the third best predictor being a highly negative tangential curvature followed closely by a highly positive profile curvature for the Normalized Landslide Index Method. By contrast, land cover and lithology are the most important variables found in the standard landslide index method.

Figure 8 represents the landslide hazard susceptibility map derived from the analysis described above. Classification of the continuous weight values was done using the cumulative distribution of those values across the domain (Fig. 6). Weight values below the 50th percentile were considered low, between the 50th and 70th medium, the 70th and 90th high, and above the 90th percentile very high.

$$\begin{aligned} \text{Low} &\leq -0.1348 \\ -0.1348 &< \text{Medium} \leq 0.01131 \\ 0.01131 &< \text{High} \leq 0.1948 \\ 0.1948 &\leq \text{Very High} \end{aligned}$$

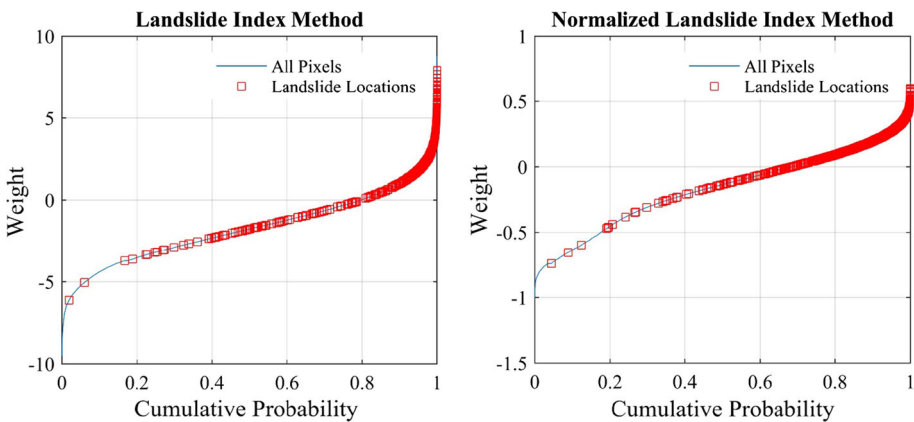


Fig. 6 Cumulative probability plots of weight values from landslide and Normalized Landslide Index Methods, indicating landslide pixel values as red boxes

Fig. 7 Variable class weights for six variables of interest from Normalized Landslide Index Method and landslide index method

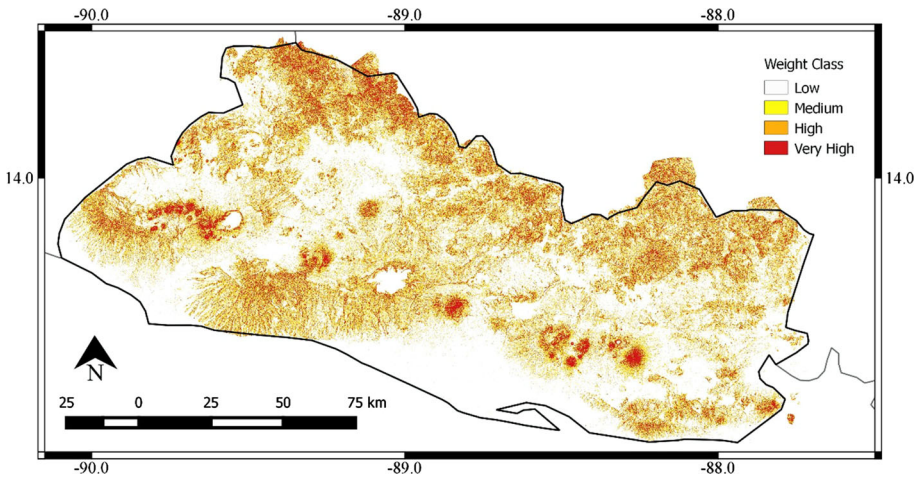
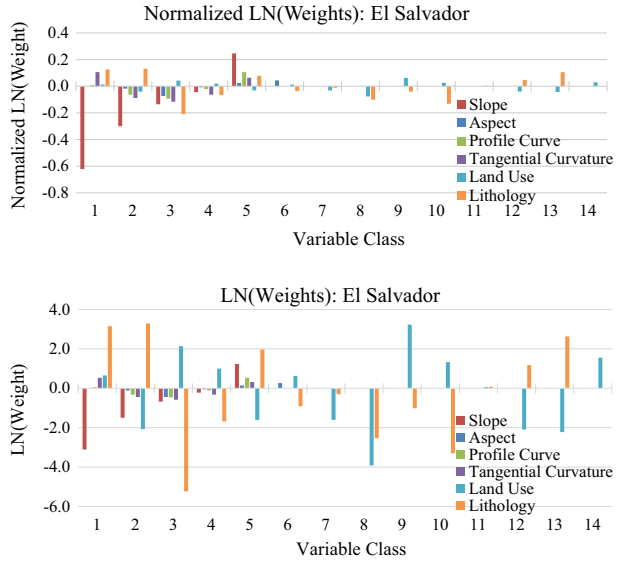


Fig. 8 Landslide susceptibility map for El Salvador from the Normalized Landslide Index Method

The map clearly shows that locations adjacent to the large volcanos and other mountain ranges, where steep slopes and unconsolidated material are most likely to be located, have the highest susceptibility.

3.3 Analytical Hierarchy Process in landslide susceptibility mapping

Many researchers have used AHP to develop weighting factors for the causative parameters and used objective analyses such as the landslide index method to develop weights for individual parameter classes (Akgun 2012; Hasekiogullari and Ercanoglu 2012; Bhatt et al.

2013). In other cases, AHP has been used to develop the causative factor and individual class weights (Long and De Smedt 2012; Kayastha et al. 2013). The Analytical Hierarchy Process (AHP) was developed at the Wharton School of Business by Thomas Saaty in the late 1970s, as a decision-making tool for handling complex, unstructured, multi-criteria decisions, allowing the incorporation of both objective and subjective considerations in the decision-making process (Yalcin 2008; Yohsimatsu and Abe 2006). Use of this decision-making strategy has become quite common for developing landslide susceptibility maps.

Saaty (1980) derived the AHP to standardize the multi-factor decision-making process, by reducing multiple variable decisions into a series of couple/pair comparisons and uses subjective priorities based upon the user’s judgment. Pair comparisons are made in an effort to determine a relative preference of each factor in accomplishing the overall goal.

Using the numerical values established in the Fundamental Saaty’s Scale (Table 7), values are assigned to each factor pair. Pair comparisons values are based on the preference of the vertical axis to the horizontal axis (Table 8). The reciprocal of each degree of preference indicates a preference for the horizontal factor over the factor on the vertical axis. Table 8 represents the values determined for those factors used in determining landslide hazard susceptibility and the pair-wise comparisons of each of those factors.

Once the factor preferences have been determined for each pair-wise comparison for those variables used to estimate relative importance for landslide susceptibility, the next step in the AHP is the arithmetic mean process. In this step, the values of each column of coupled comparisons are summed. Then, the values of each cell of the pair-wise comparison matrix are divided by the summed value of the same factor column, and finally, the factor mean values are derived in each row as an arithmetic average of the values in each row (Table 9).

The AHP mean values were then multiplied by the factor weight class values derived from the landslide index method according to Eq. (2) (Bhatt et al. 2013).

$$M = \sum_{i=1}^n Y_i * X_i \tag{2}$$

where, *M*, cumulative weight value = susceptibility coefficient; *X_i*, factor class weight derived from quantitative assessment of landslide hazard susceptibility (e.g., normalized landslide hazard index); and *Y_i*, the AHP-derived weight value for each landslide susceptibility factor.

Table 8 Matrix shows the pair comparisons for each factor

	Slope	Aspect	Tangential curvature	Profile curvature	Lithology	Land cover
Slope	1.0000	9.0000	9.0000	9.0000	7.0000	7.0000
Aspect	0.1111	1.0000	0.2000	0.3333	0.1667	0.3333
Tangential curvature	0.1111	5.0000	1.0000	4.0000	0.2000	0.2000
Profile curvature	0.1111	3.0000	0.2500	1.0000	0.1429	0.2500
Lithology	0.1429	6.0000	5.0000	7.0000	1.0000	3.0000
Land cover	0.1429	3.0000	5.0000	4.0000	0.3333	1.0000
Sum	1.6190	27.0000	20.4500	25.3333	8.8429	11.7833

Bold values indicate input values according to Saaty’s scale. Decimal values are reciprocals, indicating preference on the vertical axis

Table 9 Second step of the Analytic Hierarchy Process is to determine the proportion of each factor by row

	Slope	Aspect	Tangential curvature	Profile curvature	Lithology	Land cover	Mean
Slope	0.6176	0.3333	0.4401	0.3553	0.7916	0.5941	0.5220
Aspect	0.0686	0.0370	0.0098	0.0132	0.0188	0.0283	0.0293
Tangential curvature	0.0686	0.1852	0.0489	0.1579	0.0226	0.0170	0.0834
Profile curvature	0.0686	0.1111	0.0122	0.0395	0.0162	0.0212	0.0448
Lithology	0.0882	0.2222	0.2445	0.2763	0.1131	0.2546	0.1998
Land cover	0.0882	0.1111	0.2445	0.1579	0.0377	0.0849	0.1207

The mean of each row is calculated and indicates the subjective preference for each factor derived from pairwise comparisons

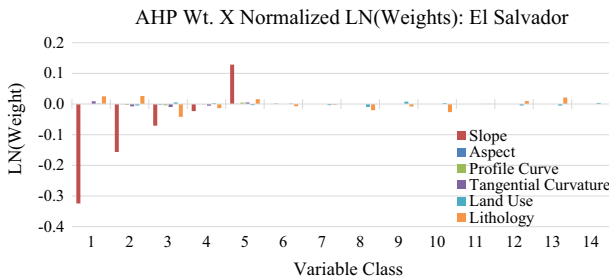


Fig. 9 Variable class weights for six variables of interest from landslide index method and then multiplied by their corresponding factor weight from AHP

Each of these values is given in Tables 1, 2, 3, 4, 5, 6 in the last column. Figure 9 is commensurate to Fig. 7, except that now each factor class weight has been multiplied by the factor weight derived from the AHP. Figure 9 illustrates that the effect of including the AHP factor weights increases the net importance of those factors already identified in the statistical analysis.

3.4 Normalized Landslide Index Method comparison with physically based method

In some cases, predetermined classes for each variable are associated with landslide susceptibility and are combined to determine overall susceptibility. In cases where there is little information on existing landslides, this is the final and only option. In cases where landslide locations are available, this strategy may still be used, and landslide locations may be used to calibrate and validate variable class susceptibility ranking. This a priori approach was undertaken by SNET in 2004, with additional factors representing the climatology and level of seismicity (SNET 2004). Figure 10 represents the analysis by the team at SNET who implemented an a priori approach to landslide hazard zonation developed in Costa Rica, C.A., by Mora and Vahrson (1991). This approach uses Eq. (3) to determine the overall susceptibility of any given grid cell in the spatial domain:

$$Susc = (S * L * P) * (Si + I) \tag{3}$$

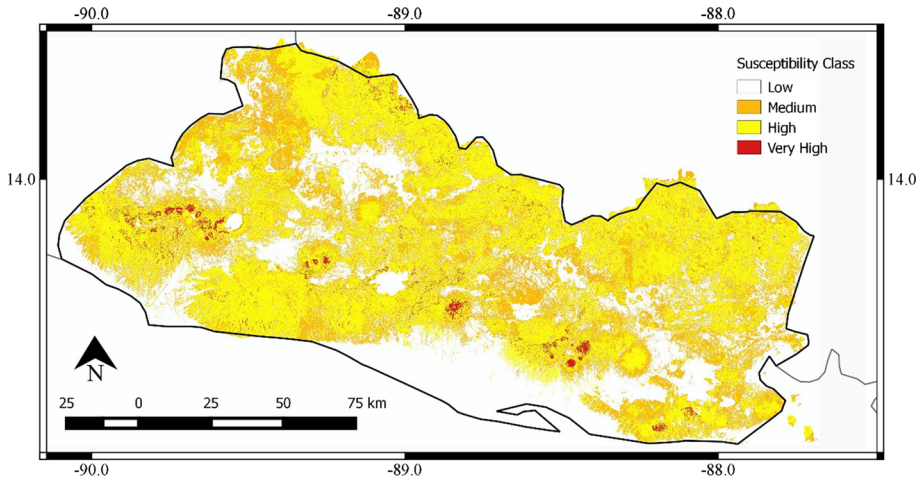


Fig. 10 Landslide susceptibility map developed by SNET using approach developed by Mora and Vahrson (1991)

where, *susc*, landslide susceptibility weight; *S*, slope index; *L*, lithology index; *P*, index of precipitation monthly averages then summed over the year; *S_i*, seismicity index based on a development regulatory map that indicates the maximum terrain acceleration in the past 100 years; *I*, rainfall intensity index based on the annual daily maximum values from rainfall recording stations, interpolated across the country.

Each factor listed above is divided into five to ten classes. The range of values for each factor class is based on the judgment of the researcher. Based on the factor class ranges, an integer weight value is assigned, where zero or one represents very low impact to landslide susceptibility, with increasing values for each subsequent factor class.

Results from the Mora–Vahrson, normalized and standard landslide index method approaches are very similar in their identification of steep slopes at high elevations on mountains and volcanos. However, Figs. 10 and 11 illustrate that the Mora–Vahrson technique identifies large areas as high susceptibility, nearly as much area as identifies as low susceptibility, and relatively little area as very high susceptibility. By contrast, the Normalized Landslide Index Method susceptibility classes are distributed based on the cumulative probability of values, whereby low values are highly represented, with the remaining classes being approximately equally represented (Fig. 11).

3.5 Susceptibility map validation

Validation of the susceptibility map development techniques is first assessed through comparison with the actual landslide locations. Given that the landslide index method susceptibility weights are derived from the landslide locations, we expect there to be an excellent correlation with high and very high susceptibility classes. An analysis of Figs. 11 and 12 shows that landslide locations are overrepresented in the expected susceptibility classes, as landslide locations are skewed toward high and very high, while all grid cell values are skewed toward medium and low susceptibility classes.

By contrast, the skew toward a large number of landslides occurring in the high susceptibility class, as derived by the Mora–Vahrson method, does not indicate success of the

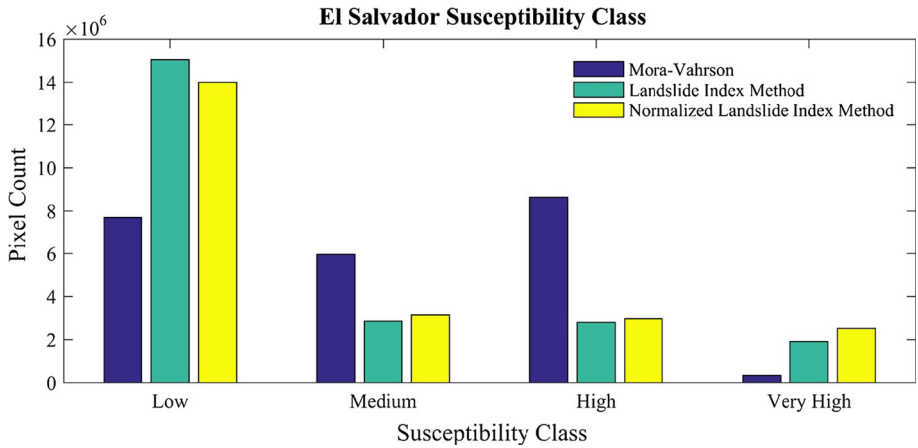


Fig. 11 Histogram of landslide susceptibility class values for the Mora–Vahrsen, landslide index method, and Normalized Landslide Index Method classification methods over El Salvador

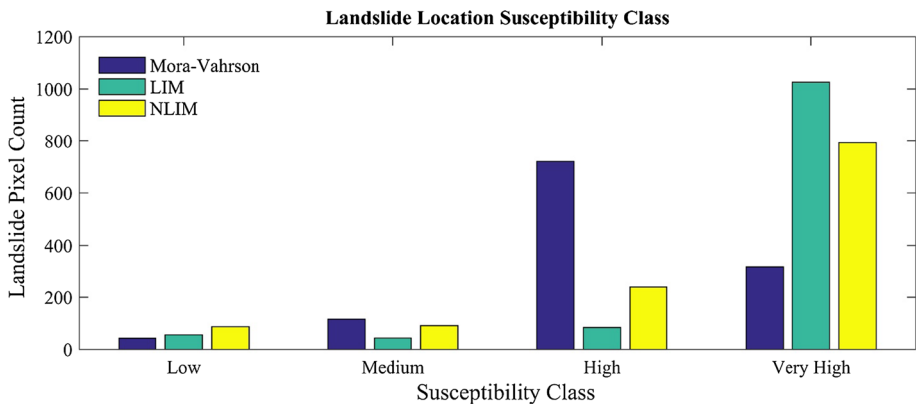


Fig. 12 Histogram of landslide events within each of the susceptibility classes, as determined by the Mora–Vahrsen and landslide index methods

method due to the disproportionately large area designated high susceptibility in that method. However, the very high susceptibility class does appear to capture very landslide-prone areas, as the number of landslide found in that class is overrepresented when compared to the number of grid cells designated very high.

AA commonly used method to validate susceptibility map development strategies is to use the receiver operating characteristics (ROC) curve (Marjanovic 2013; Frattini et al. 2010). The ROC curve represents a validation metric that illustrates the relative trade-offs between the benefits and costs of moving the threshold which describes the hit or miss of a model, i.e., the true-positive rate (tp_{rate} or hit rate) and the false-positive rate (fp_{rate} or false alarm rate). These rates are determined through development of a contingency table (Table 10) at given probability threshold intervals, or scoring scales. The most common numeric metric of evaluation in ROC space is the area under the curve (AUC). The closer the AUC is to 1 (within the 0–1 span), the better the performance.

Table 10 Contingency table and ROC space coordinates

		Landslide inventory		ROC space coordinates
		True	False	
Model	Positive	tp (true positive)	fp (false positive)	$tp_{rate} = tp/(tp + fn)$
	Negative	fn (false negative)	tn (true negative)	$fp_{rate} = fp/(fp + tn)$

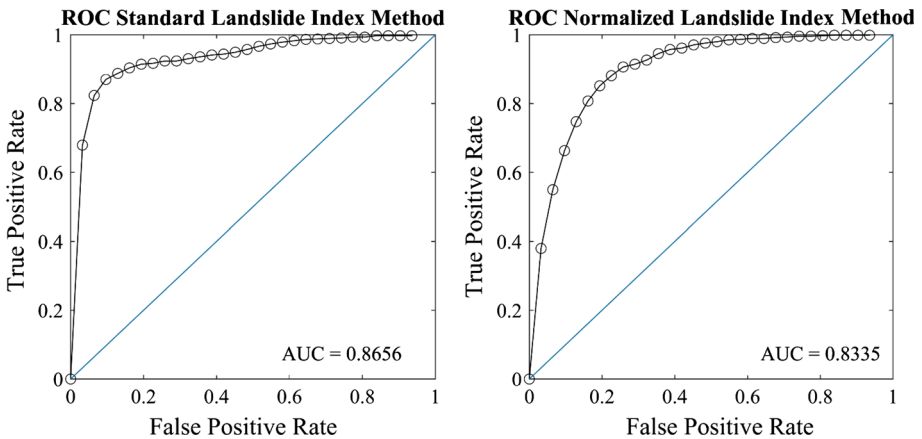


Fig. 13 Receiver operating characteristics curves and area under the curve values for both standard and Normalized Landslide Index Method

This validation strategy required the landslide observation dataset to be divided into training and test subsets. Of the 545 landslide polygons delineated, 232 were used as the training dataset and 313 were used for the test dataset. Polygons were chosen randomly across the domain. Figure 13 illustrates the ROC curves and AUC values for both the standard and Normalized Landslide Index Methods. The AUC values are nearly identical and very good for both methods, with the standard method being slightly better.

4 Discussion

Derivation of a landslide susceptibility map for El Salvador using the point locations of landslides provided by in-country agencies and the standard landslide index method resulted in several findings that were inconsistent with expectations based on known factors controlling shallow landslide locations. These finding led to various enhancements of the initial strategy. Foremost is the further investigation and validation of landslide locations and their transfer from being represented as points to their representation as polygons, providing a more robust representation of landslide spatial distribution in the domain. This effort resulted in variable weights that were more consistent with expectations. However, inspection of variables that were most important in predicting landslide susceptibility led to the discovery that the largest variable class weights were associated with lithology and land cover. Using the standard landslide index method, the largest variable class weights within the lithology and land cover variables were nearly three times

as large as the largest weights found in the slope variable. This discovery led to the determination that due to the number of classes within those variables, being much greater than classes delineated within continuous variables associated with DEM-derived products, landslides locations were more likely to be overrepresented in one class. Therefore, normalization of the class weights based on the number of classes within that variable redistributed class weights across variables resulting in a more evenly divided distribution of weights across variables, along with the finding that slope is the most important factor in determining landslide susceptibility.

Normalization of the variable classes also has a dramatic impact on the distribution of continuous values (Fig. 6). The shorter tails and more even distribution associated with the normalization process mean that fewer values are found at the extremes of the distribution. Therefore, when classifying the continuous values based on the cumulative distribution (i.e., greater than 90th percentile indicating very high susceptibility), a wider range of values are found in this class. This fact results in the findings illustrated in Fig. 12, where the standard landslide index method captures more landslides in the very high class than the Normalized Landslide Index Method.

Classification of continuous values and the overall weight totals strongly determines the importance of any given variable. There is no standard methodology for classifying continuous values in the derivation of landslide susceptibility maps. Several iterations were completed in developing the methodologies presented herein. With respect to classification of variables, the implementation of five equal bin sizes for classification resulted in the third class representing a planar or mean class. Inspection of Tables 3 and 4 illustrates that this third bin does represent a planar class, as values fall into a range above and below zero. Inspection of Table 1 classification finds that the extreme slope class begins at approximately 18° . This classification is consistent with expectations for steep to mild slopes.

Classification of overall susceptibility weights was also completed over several iterations. The use of the cumulative distribution to classify this continuous variable was both logical and resulted in the capture of landslide locations in each susceptibility class at rates consistent with expectations. This step in the process is an important determinant on how conservative or liberal a susceptibility map is and therefore represents its utility. Having large areas of high and very high susceptibility class may do an excellent job at capturing landslide locations, but is not very informative for decision-making as, for example, too many areas are eliminated from potentially useful land uses. In contrast, small of areas in high and very high susceptibility classes may not capture areas that have a high threat of landsliding. This may be the case for the classification used in the development of the Mora–Vahrson susceptibility map. Unfortunately, for this work the authors were provided only the final classified map and not the continuous weights derived from their analysis; therefore, we were unable to assess how classification was done and what impact it may have had on the distribution of weights both across the domain and at landslide locations.

The Analytical Hierarchy Process resulted in a slightly different ordering of variable importance. Based on the AHP strategy, slope is the most important variable, followed by lithology, land cover, tangential, profile curvature, and lastly aspect. This ordering is very similar to the findings of the Normalized Landslide Index Method that also found slope to have the highest positive association with landsliding, followed by lithology, profile, tangential curvature, land cover, and then aspect. The finding that these two methods result in a similar association with landslide susceptibility supports the need for normalization. The standard landslide index method found lithology to be the most important factor, followed by land cover, slope, profile, tangential curvature, and lastly aspect.

The relative distributions of the number of pixels in each susceptibility class across the entire domain compared to the number of landslides in a given susceptibility class provide some insight into the skill of the model to detect landslide susceptibility. Normalization of variable class weights reduces the number of total pixels in the low class and increases the number of pixels in the very high class, relative to the standard method. This distribution change is not consistent when looking in which class landslides occurred. Landslides are overwhelmingly represented in the very high class of the standard method, with the remaining landslides being nearly evenly divided between the other classes. In contrast, the normalized method results in fewer landslides in the very high class, with the remaining landslides reducing in number with reduced susceptibility. Distribution of susceptibility class using the Mora–Vahrson method has two peaks in both the low and high class, having slightly fewer medium and very little area in the very high class. Distribution of landslides using the Mora–Vahrson method shows that the high and very high classes capture the majority of landslides, where the number of landslides in the high class is nearly double that of the very high class. Results from the ROC curve analysis show little difference between the two methods, suggesting that the both have similar reliabilities; however, ROC curves do not indicate accuracy of the methods tested.

5 Conclusions

The Normalized Landslide Index Method is a statistically based method that relies on a landslide inventory map along with maps of other relevant factors including DEM-derived parameters such as slope, aspect, and profile and tangential curvatures, as well as lithology, land use, and road network. Normalizing the weights derived for each factor class, by the number of classes in that factor, eliminates the importance of the number of classes for any given factor. This conclusion was derived from the development of previous iterations of this analysis that showed a significantly reduced importance of lithology and land use factors due to the large number of classes. Normalization of variable class weights results in a more conservative approach to delineating landslide susceptibility by creating a more even distribution of weights and reducing the number of values, which represent areal extent, of extreme weight values across the domain.

The result of this analysis also suggests that implementation of the AHP method in conjunction with another statistical or physically based landslide susceptibility determination strategy, may reduce the effect of lower susceptibility factor classes and increase the effect of higher susceptibility factor classes, as was the case when combined with the normalized results. However, in other cases inclusion of the AHP factors may mitigate unexpected results by increasing the weight of factors whose significance is known to be high, such as the case of standard landslide index method results. These impacts may be determined to be advantageous or not by individual researchers in different regions. In El Salvador, it was determined that incorporation of the AHP method diluted the results of the Normalized Landslide Index Method and was therefore not used in development of the final susceptibility map.

Finally, the physically based susceptibility map provided by SNET, as a result of the Mora–Vahrson method, makes for an excellent opportunity to compare the two methods. The Mora–Vahrson method results indicate that large portions of the area are in the high susceptibility class, including areas with low percent slopes, whereas large areas around the high-altitude slopes of the volcanos and other mountains are classified as only medium

or high susceptibility. This is at least in part due to the linear relationship presented in Eq. (3). This relation does not account for the number of classes in any given factor and treats all factors the same. For example, the annual daily precipitation maximum and rainfall intensity weights are both from 0 to 5, which results in areas of high rainfall accumulating high susceptibility weights in very unlikely areas due to the absence of steep slopes. By contrast, the Normalized Landslide Index Method relies solely on the landslide location data that may not be representative of all of the areas where landslides are likely to occur. This work supports the conclusion by Hervás et al. (2013) that rather than focusing on the comparison of different statistical models, more attention should be paid to improve the selection and preprocessing of the input variables because this has probably much more effect on the model results than the statistical model used. However, implementation of a statistical model is superior to its a priori physically based counterpart. In addition, normalization of the standard landslide index method results in a more conservative approach and more convincing overall landslide susceptibility map.

Acknowledgments The authors are thankful to the UN World Meteorologic Organization and the US Agency for International Development for the support of this project. Additional support was provided by the Technology Transfer Program of the Hydrologic Research Center. The authors would also like to thank the staff at SNET (Mario Reyes and Manuel Diaz), El Salvador, for their cooperation in providing data, maps, references, and details about specific landslide events. This work could not have been accomplished without their help.

References

- Aguilar M, Pacheco T, Tobar J, Quiñónez J (2009) Vulnerability and adaptation to climate change of rural inhabitants in the central coastal plain of El Salvador. *Clim Res* 40(2–3):187–198
- Akgun A (2012) A comparison of landslide susceptibility maps produced by logistic regression, multicriteria decision, and likelihood ratio methods: a case study at Izmir, Turkey. *Landslides* 9:93–106
- Ayalew L, Yamagishi H (2005) The application of GIS-based logistic regression for landslide susceptibility mapping in the Kakuda-Yahiko Mountains, Central Japan. *Geomorphology* 65:15–31
- Ayalew L, Yamagishi H, Marui H, Kanno T (2005) Landslides in Sado Island of Japan: part II. GIS-based susceptibility mapping with comparisons of results from two methods and verifications. *Eng Geol* 81:432–445
- Baxter S (1984) *Lexico Estratigrafico De El Salvador*. Comision Ejecutiva Hidroelectrica Del Rio Lempa, San Salvador, El Salvador
- Bell GD, Halpert MS, Ropelewski CF, Kousky VE, Douglas AV, Schnell RS, Gelman ME (1999) Climate assessment for 1998. *Bull Amer Meteor Soc* 80:S1–S48
- Bhatt BP, Awasthi KD, Heyojoo BP, Silwal T, Kafle G (2013) Using geographic information system and analytical hierarchy process in landslide hazard zonation. *Appl Ecol Environ Sci* 1(2):14–22
- Carrara A, Cardinali M, Guzzetti F, Reichenbach P (1995) GIS technology in mapping landslide hazard. In: Guzzetti F, Carrara A (eds) *Geographical information systems in assessing natural hazards*. Kluwer Academic, Dordrecht, pp 135–175
- Cevik E, Topal T (2003) GIS-based landslide susceptibility mapping for a problematic segment of the natural gas pipeline, Hendek (Turkey). *Environ Geol* 44:949–962
- Dai FC, Lee CF, Li J, Xu ZW (2001) Assessment of landslide susceptibility on the natural terrain of Lantau Island. *Hong Kong Environ Geol* 43(3):381–391
- Dai FC, Lee CF, Ngai YY (2002) Landslide risk assessment and management: an overview. *Eng Geol* 64(1):65–87
- Ercanoglu M, Gokceoglu C (2004) Use of fuzzy relations to produce landslide susceptibility map of a landslide prone area (West Black Sea Region, Turkey). *Eng Geol* 75(3/4):229–250
- Frattoni P, Crosta G, Carrara A (2010) Techniques for evaluating the performance of landslide susceptibility models. *Eng Geol* 111:62–72
- GRASS Development Team (2012) Geographic resources analysis support system (GRASS) software. Open Source Geospatial Foundation Project. <http://grass.osgeo.org>

- Hasekiogullari GD, Ercanoglu M (2012) A new approach to use AHP in landslide susceptibility mapping: a case study at Yenice (Karabuk, NW Turkey). *Nat Hazards* 63(2):1157–1179
- Hellin J, Haigh H, Marks F (1999) Rainfall characteristics of Hurricane Mitch. *Nature* 399:316
- Kayastha P, Dhital MR, De Smedt F (2013) Application of the analytical hierarchy process (AHP) for landslide susceptibility mapping: a case study from the Tinau watershed, west Nepal. *Comput Geosci* 52:398–408
- Komac M (2006) A landslide susceptibility model using the analytical hierarchy process method and multivariate statistics in perialpine Slovenia. *Geomorphology* 74(1–4):17–28
- Lan HX, Zhou CH, Wang LJ, Zhang HY, Li RH (2004) Landslide hazard spatial analysis and prediction using GIS in the Xiaojiang watershed, Yunnan. *China Eng Geol* 76(1–2):109–128
- Lee S, Min K (2001) Statistical analysis of landslide susceptibility at Yongin. *Korea Environ Geol* 40:1095–1113
- Lee S, Choi J, Min K (2004a) Probabilistic landslide hazard mapping using GIS and remote sensing data at Boun. *Korea Int J Remote Sens* 25(11):2037–2052
- Lee S, Ryu J, Won J, Park H (2004b) Determination and application of the weight for landslide susceptibility mapping using an artificial neural network. *Eng Geol* 71:289–302
- Long NT, De Smedt F (2012) Application of an analytical hierarchical process approach for landslide susceptibility mapping in A Luoi district, Thua Thien Hue Province. *Vietnam Environ Earth Sci* 66(7):1739–1752
- Marjanovic M (2013) Comparing the performance of different landslide susceptibility models in ROC space. In: Margottini C, Canuti P, Sassa K (eds) *Landslide science and practice volume 1: landslide inventory and susceptibility and hazard zoning*. Springer, Berlin, p 607
- MATLAB and Statistics Toolbox Release (2012). The MathWorks Inc, Massachusetts
- Meisina C, Zizioli D, Zucca F (2013) Methods for shallow landslides susceptibility mapping: an example in Oltrepo Pavese. In: Margottini C, Canuti P, Sassa K (eds) *Landslide science and practice volume 1: landslide inventory and susceptibility and hazard zoning*. Springer, Berlin, p 607
- Microsoft (2010) Microsoft excel, redmond: microsoft (2010) computer software, Washington
- Mora S, Vahrson W (1991) Determinación a Prior de la Amenaza de Deslizamientos in Grandes Áreas y Utilizando Indicadores Morfodinámicos. Universidad de Costa Rica y Universidad Nacional de Costa Rica. Julio, Instituto Costarricense de Electricidad, Costa Rica
- Parise M (2001) Landslide mapping techniques and their use in the assessment of the landslide hazard. *Phys Chem Earth Part C* 26(9):697–703
- Pasch RJ, Avila LA, Jiing J (1998) Atlantic tropical systems of 1994 and 1995: a comparison of a quiet season to a near-record breaking one. *Mon Weather Rev* 126:1106–1123
- Perotto-Baldoviez HL, Fisher RF, Wu XB, Thurow TL, Smith CT (2004) GIS-based spatial analysis and modeling for landslide hazard assessment in steeplands, Southern Honduras. *Agric Ecosyst Environ* 103(1):165–176
- QGIS Development Team (2014) QGIS Geographic Information System. Open Source Geospatial Foundation Project. <http://qgis.osgeo.org>
- Quinn PE, Hutchinson DJ, Diederichs MS, Rowe K (2010) Regional-scale landslide susceptibility mapping using weights of evidence method: an example applied to linear infrastructure. *Can Geotech J* 47:905–927
- Rautela P, Lakhera RC (2000) Landslide risk analysis between Giri and Ton Rivers in Himalaya (India). *Int J Appl Earth Obs Geoinform* 2:153–160
- Rose WI, Bommer JJ, Sandoval C, Carr MJ, Majors JJ (2004) Natural hazards in El Salvador. *Geologic Society of America of Special Paper* 375, Boulder
- Saaty TL (1980) *The Analytical Hierarchy Process*. McGraw Hill, New York
- SNET (2004) Memoria Técnica Para el Mapa de Susceptibilidad de Deslizamientos de Tierra en El Salvador. Servicio Nacional de Estudios Territoriales, Ministerio de Medio Ambiente y Recursos Naturales, El Salvador
- Van Den Eeckhaut M, Vanwalleghem T, Poesen J, Govers G, Verstraeten G, Vandekerckhove L (2006) Prediction of landslide susceptibility using rare events logistic regression: a case-study in the Flemish Ardennes (Belgium). *Geomorphology* 76:392–410
- Van Westen CJ (1997) Statistical landslide hazard analysis, ILWIS application guide 5: 73–84. ITC, Enschede
- Yalcin A (2008) GIS-based landslide susceptibility mapping using analytical hierarchy process and bivariate statistics in Ardesen (Turkey): comparisons of results and confirmations. *Catena* 72:1–12
- Yohsimatsu H, Abe S (2006) A review of landslide hazards in Japan and assessment of their susceptibility using an analytical hierarchic process (AHP) method. *Landslides* 3:149–158
- Zêzere JL (2002) Landslide susceptibility assessment considering landslide typology, a case study in the area north of Lisbon (Portugal). *Nat Hazard Earth Syst Sci* 2:73–82